Biochimica et Biophysica Acta, 777 (1984) 167–182
Elsevier

BBA 72289

LARGE-LIGAND ADSORPTION TO MEMBRANES

III. COOPERATIVITY AND GENERAL LIGAND SHAPES

STEFAN STANKOWSKI

Biozentrum der Universität, Klingelbergstrasse 70, 4056 Basel (Switzerland)

(Received April 26th, 1984)

Key words: Membrane-ligand interaction; Binding isotherm; Cooperativity; Ligand incorporation; Polymyxin

In previous reports (Stankowski, S. (1983) Biochim. Biophys. Acta 735, 341–351 and 352–360) the ordinary Scatchard-type analysis has been shown to yield erroneous results when applied to the binding of large molecules to membranes or cells. Formulae have been given to treat the limiting cases of very thin and of very bulky ligands. These results are now extended to include ligands of any shape and cooperative interactions. As an example, data on the cooperative binding of polymyxin to charged lipid bilayers are reevaluated. Adsorption with concomitant incorporation of the large molecule into the membrane is also considered.

Introduction

In the present series of articles, we try to construct a suitable formalism for the evaluation of ligand binding to an array of binding contacts on a surface (membrane). Special emphasis is given to the steric effects which arise with large ligands covering more than one binding contact upon adsorption. In the following, we assume that each 'binding site' for a ligand molecule is made up of n binding contacts, with $n > 1$.

In the previous reports [1,2], it has been shown that the common practice of setting the concentration of free sites equal to that of free contacts divided by n, is inadequate. To see this, consider, for example, the binding of $n = 2$ ligands ('dimers') to a square lattice of contacts: at vanishing surface saturation, there are $2N$ possibilities (and not $N/2$) to place a dimer on a lattice composed of N contacts: namely , N horizontal and N vertical arrangements. (We neglect end-effects assuming that N is very large or that the surface is closed as on a vesicle.) The number of free sites tends to half the number of free contacts only in the limit of maximum saturation (as is obviously true for the last free site on a nearly saturated surface). This example is of relevance for the 1 : 2 binding of divalent ions to lipid membranes. A critique of the wrong use of the mass-action law along with a correct calculation of the Grahame equation for divalent ion adsorption have been published recently [3].

The difference between the wrong and the correct isotherms is most easily visualized by plotting them according to Scatchard [4]: setting [free sites] = [free contacts]/n obligatorily yields straight-line Scatchard plots, whereas the correct treatment results in binding curves which are bent downwards, at least if the binding is not cooperative. (Experimental Scatchard binding curves may nevertheless appear quite straight if data are available only from a limited range of concentrations; use of the conventional evaluation procedures may then yield parameter values which are grossly in error.) Scatchard plots which are curved downwards must therefore not always reflect the superposition of

0005-2736/84/$03.00 © 1984 Elsevier Science Publishers B.V.

several binding modes [5] or true anticooperative interactions [6], but may simply represent the steric constraints of large ligands [6]. The quantitative degree of downward curvature has been shown to depend crucially on the size and shape of the ligand molecules [2]. Suitable formulae have previously been given to treat the special cases of very thin, stretched ligands [1] (using the approximation scheme of Miller and Guggenheim [7]), and of bulky, fully symmetric ligands [2] (adapting the hard sphere model of Andrews [8]). These two cases represent extremes, in the sense that the former yields the most strongly, the latter the least strongly curved Scatchard plots for a given stoichiometric number n.

In the present article, these results have been extended to more general ligand shapes, using a simple extrapolation formula. Cooperative effects are also included. Published data on peptide binding to lipid membranes have been reevaluated for demonstration.

The emphasis is again on the steric properties of large ligands (correct counting of free sites, excluded areas, etc.). We are less interested in problems arising from the flexibility of long-chain polymers which have found considerable attention in polymer chemistry (see, e.g., Refs. 9 and 10 and references therein). Instead our treatment refers essentially to molecules with well-defined conformations such as proteins (conformational changes upon binding are not excluded). In contrast to the problem of random sequential adsorption [11,12], we are dealing with an equilibrium situation where the adsorbed molecules do not stick irreversibly but can rearrange by lateral diffusion and/or desorption and readsorption processes.

Very recently, a treatment of surface adsorption of thin stretched ligands has been published by Miyazawa [13] along the lines of Guggenheim's theory [7,14]. It is equivalent to ours [1], and already includes cooperativity and binding of more than one ligand species. Miyazawa's treatment is limited, however, to what we call linear ligands. In comparison to Miyazawa's work, our efforts have mainly been directed towards inlcuding more general ligand shapes and building the formalism on a particularly simple and transparent mathematical basis. We think that the latter point is quite important for the following two reasons. Firstly, we address ourselves mainly to practical workers looking for a suitable strategy for data evaluation. Secondly, adaptation of the model to slightly different situations becomes much easier if the various expressions and parameters do not remain formal, but if their physical meaning appears in a clear and intuitive fashion. As an example, some aspects of protein incorporation into membranes have been formulated in Appendix 2.

The following sections are devoted to the derivation of the formalism. The Discussion section then gives an overlook from a more practical point of view, indicating possible applications and limitations of the model, suggesting evaluation strategies and showing up simplifications which arise in many special situations.

The basic model

Definitions and concepts underlying our treatment have been discussed extensively in the previous reports [1,2]. Here, we shall therefore limit ourselves to sketch the main ideas. We consider a regular array of binding contacts (subunits) arranged on a surface which is either closed (as on a cell or vesicle) or large enough that end-effects may be neglected. The array of contacts is characterized by its coordination number, z, i.e., the number of nearest neighbours surrounding each subunit. All contacts are presumed to be equivalent with respect to their ligand-binding properties. Lateral diffusion on the surface is not excluded as long as the contact distribution remains homogeneous (see Discussion for further comments) and the notions of number of contacts covered by a ligand molecule and shape of a ligand-bound region remain well-defined.

Equilibrium binding of ligand molecules is thought to occur in a single binding mode, each molecule covering n subunits in a defined spatial arrangement. In the following, we refer to the stoichiometric number n as to the size of a binding site and to the spatial arrangement as to its shape.

Designating the fractions of free and bound contacts by x_1 and x_2, respectively, ($x_1 + x_2 = 1$), it is easily seen that the fraction of bound sites equals:

$$r = x_2/n \qquad (1)$$

which is also identical to the degree of binding, i.e., the concentration of bound ligand divided by the total concentration of contacts. On the other hand, the fraction of free sites is not equal to x_1/n (cf. Introduction). In fact, the whole problem resides in the correct calculation of the fraction of free sites of size n (in the following designated by $x_{(n)}$).

To perform this calculation, we use the simplest approximation scheme (the doublet closure) which still accounts for the ligand shape. The method consists in reducing all distributions to those of nearest neighbour pairs. We therefore introduce fractions of free-free pairs, x_{11}, free-bound pairs, $x_{12} = x_{21}$, and bound-bound pairs, x_{22}. These are related by the following constraints:

$$x_1 = x_{11} + x_{12}$$

$$x_2 = x_{22} + x_{12} \qquad (2a,b)$$

x_{22} can be divided into two classes: x_{22}^{i} describes pairs of subunits at the interior of bound ligands, whereas x_{22}^{e} describes pairs at the edges, i.e., nearest-neighbour contacts between different ligand molecules (cf. Fig. 2 of Ref. 1). Subtracting x_{22}^{i} from Eqn. 2b and introducing a new parameter, $\lambda = (1 - x_{22}^{i}/x_2)$, we obtain:

$$\lambda x_2 = x_{22}^{e} + x_{12} \qquad (3)$$

λ is completely defined by the geometry of the binding site. It equals the number of pairs across the edges, divided by zn [1]. Values of λ for various shapes are listed in Appendix 1.

The pair fractions (which may also be interpreted as pair probabilities) are indicative of the cooperativity of the system. In the case of cooperativebinding, free subunits and bound ligands each form clusters, resulting in large x_{11} and x_{22}^{e}, but small x_{12}. On the other hand, anticooperative binding favours x_{12} at the expense of x_{11} and x_{22}^{e}. The intermediate case of purely random adsorption is characterized by the condition that the probability of finding one free-free and one bound-bound pair is equal to that of finding two mixed free-bound pairs. In general, one may write:

$$x_{11}x_{22}^{e} = x_{12}^{2}\eta \qquad (4)$$

where the parameter η indicates the degree of cooperativity: $\eta > 1$ means positive cooperativity, $\eta < 1$ anticooperativity and $\eta = 1$ random adsorption (no cooperativity). Inserting from Eqns. 2a and 3, Eqn. 4 can be solved to yield:

$$x_{12} = \frac{\lambda x_1 x_2}{x_1 + \lambda x_2}\frac{2}{\sqrt{}+1} \qquad (5)$$

with:

$$\sqrt{} = \left[1 + 4(\eta - 1)\lambda x_2(1 - x_2)/(1 - (1 - \lambda)x_2)^2\right]^{1/2} \qquad (6)$$

x_{11} and x_{22}^{e} can then be obtained immediately, again using Eqns. 2a and 3. For noncooperative adsorption, the square root, Eqn. 6, and consequently, the second factor in Eqn. 5 become unity (cf. Ref. 1, Eqn. 20).

According to Guggenheim [7], the fraction of free sites, $x_{(n)}$, can be constructed for ligands covering a linear sequence of n contacts without forming closed loops (stretched linear ligands) [1]: the probability x_1 to find the first free subunit is multiplied by a conditional probability x_{11}/x_1 for each pair in the sequence. The result is finally multiplied by a statistical factor ρ, equal to the number of distinct ways the ligand molecule can be placed on the lattice with one point held fixed. (This is the factor 2 appearing in the example given in Introduction. In general, ρ is equal to the lattice coordination number, divided by the symmetry number describing the orientational symmetry of the ligand with respect to the lattice axes; see Ref. 1 for examples.) Thus:

$$x_{(n)} = \rho x_1 (x_{11}/x_1)^{n-1} \qquad (7)$$

Note that $x_{(n)}$ results as a function of the degree of membrane saturation, $\theta = x_2$ (or, equivalently, of the degree of ligand binding, $r = x_2/n$), since x_{11} can be expressed by x_2 by means of Eqn. 5, and $x_1 = 1 - x_2$.

Binding curves have already been determined in the case of random adsorption [1]. Using the correct and general form of the mass-action law:

$$K_b c_A = r/x_{(n)} \qquad (8)$$

(K_b = binding constant; c_A = concentration of free

ligand) together with Eqns. 2–7, we obtain:

$$Kc_A = \frac{r}{1-nr}\left[\frac{1-(1-\lambda)nr}{1-nr}\right]^{\gamma} \tag{9}$$

or, in the Scatchard representation:

$$r/c_A = K(1-nr)[\ldots]^{-\gamma} \tag{10}$$

where the content of the square bracket is the same in both equations. The statistical factor ρ has been included in the binding constant ($K = K_b\rho$) and γ is given by:

$$\gamma = n - 1 \text{ (linear ligand)} \tag{11}$$

(Note that K is the same as the effective binding constant K_{eff} introduced in the previous studies [1,2]. Here, we have dropped the subscript in order to make notation easier.)

Before going over to cooperative systems, we shall first discuss an extension to nonlinear ligand shapes.

Non-linear ligands

Unfortunately, when trying to extend the results, Eqns. 9 and 10, to more general ligand shapes, one gets into conflict with the basic assumption of independent pairs (doublet closure). In fact, nonlinear structures always include some correlated pairs. Consider, for instance, the hexagon shown in Fig. 1. It contains a sequence of $(n-1)$ primary pairs, given as full lines, and a certain number of additional secondary pairs which arise automatically once the full lines are drawn (dashed bond lines in Fig. 1). Thus, the total number of pairs, generally given [1] by $zn(1-\lambda)/2$, is larger than $(n-1)$ for all but linear ligands.

Consequently, it is not clear what power to use for (x_{11}/x_1) in the construction of $x_{(n)}$, or, equivlently, what to take for the parameter γ in Eqns. 9 and 10. In order to be consistent with respect to the assumption of independent pairs, $\gamma = zn(1-\lambda)/2$ would be appropriate, but this choice would not account for the difference between primary and secondary pairs. Alternatively, we may set $\gamma = (n-1)$, as before, giving a weight of unity to the secondary pairs because they arise automatically.

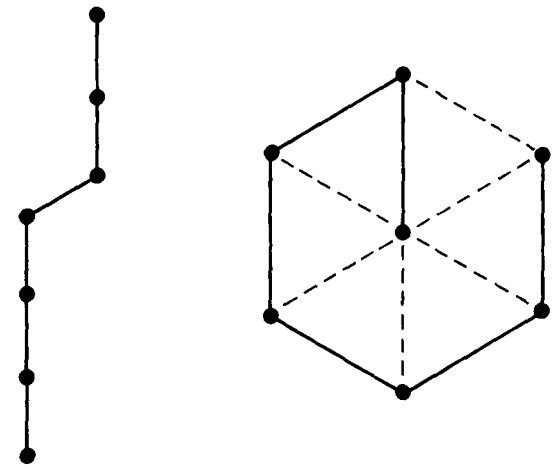

Fig. 1. The total number of pairs, indicated by bond lines between neighbouring lattice points, equals $n-1$ only for linear structures. For the compact regular hexagon, secondary bonds (------) arise automatically once the $n-1$ primary bonds (———) are drawn.

Neither of these assignments gives satisfactory results as can be checked easily by looking at the initial slopes of the corresponding Scatchard curves. These initial slopes S_0 are easily obtained [1] by differentiating Eqn. 10:

$$S_0 = -nK(1+\gamma\lambda) \tag{12}$$

On the other hand, their exact values can be calculated from a virial expansion, as demonstrated in Ref. 2:

$$S_0 = -nK(1+\alpha) \tag{13}$$

where the parameter α is the excluded area of the ligand, divided by n (see Ref 2 for more details). Comparison of Eqns. 12 and 13 suggests to try an empirical way out of the dilemma, namely to reinterpret γ in terms of the excluded area. We therefore define:

$$\gamma = \alpha/\lambda \tag{14}$$

for ligands of general shapes. For linear rods, Eqn. 14 reduces to $\gamma = (n-1)$, as before. Note that the generalization of the linear-ligand theory given by Eqn. 14 is empirical, in the sense that it cannot be justified consistently in the framework of the Miller-Guggenheim model. However, the new

parameter α entering through Eqn. 14 is not experimental, but can be predicted by purely geometrical considerations. Values of α and λ have been compiled for a number of ligand shapes in Appendix 1. For still other shapes, they can be determined easily according to the recipes given in Refs. 2 and 1.

Inserting the appropriate $\gamma = \alpha/\lambda$ into Eqns. 9 and 10 yields binding curves of remarkable precision. Some Scatchard plots calculated in this way are shown in Fig. 2, and compared with the results of numerical Monte Carlo simulations. The latter were performed by taking advantage of the Scatchard-type representation which is equivalent to plotting the number of remaining free sites as a function of the degree of saturation. Thus, structures of a given shape were added randomly to a 150×150 lattice with periodic boundary conditions. After the desired degree of saturation of the lattice was attained, a large number of additional desorption/adsorption steps was used to equilibrate the spatial arrangement of the ligands. At each step, the number of remaining free sites was determined. The results are supposed not to depend on the lattice size, since they were found not to be sensitive to a reduction of the lattice to 100×100 points.

Since our empirical formula has been established as an extrapolation, starting from the case of linear ligands, we presume that it will work best for thin, near-to-linear shapes and worst for bulky, symmetric shapes. In Fig. 2, we therefore concentrated on the worst case. It appears, however, that the accuracy remains fully sufficient for practical needs, even in the case of hexagons on a hexagonal lattice.

In fact, in the latter case, the discrepancies are still small compared to what would result from minor changes of the shape away from idealized symmetry. For demonstration, Fig. 3 depicts the Scatchard curve for a structure obtained by adding one neighbouring point to an $n = 7$ hexagon. The resulting arrow-head pentagon has parameter values $n = 8$, $\lambda = 5/12$ and $\alpha = 91/48$. The discrepancy between the corresponding isotherm and that of the hexagon is significantly larger than the deviations between the calculated hexagon curve and the Monte Carlo simulation. Similarly, we have verified that the differences between calculated and simulated isotherms for a 5×5 square are definitely smaller than those between the binding curve of the square and of a structure obtained by adding a single lattice point to it. In the latter example, the deviations are too small to be shown in a line drawing.

Fig. 2 also presents isotherms calculated according to the extended and simplified model of Andrews [2], valid for fully symmetric shapes (dashed lines). Apart from the hexagon curve, the

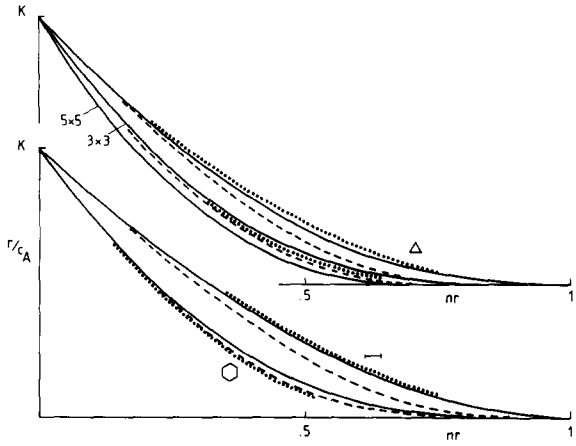

Fig. 2. Monte Carlo simulations (· · · · · ·) are compared to calculated isotherms according to Eqn. 10 (———) and to Eqn. 16 of Ref. 2 (------). Lower panel: dimers ($n = 2$) and hexagons ($n = 7$) on hexagonal lattice.Upper panel: triangle ($n = 3$) on hexagonal lattice and 3×3 and 5×5 squares on square lattice. For the 5×5 square, the three calculations agree too closely to be separated in the diagram.

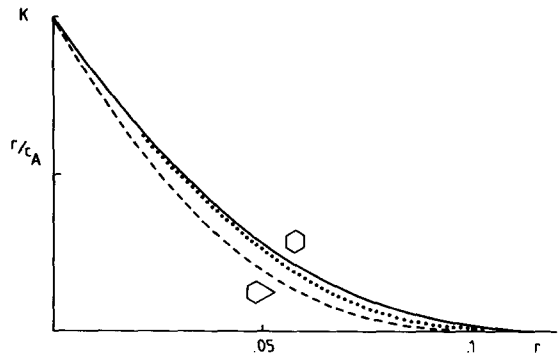

Fig. 3. Comparison of the isotherms of a hexagon ($n = 7$) and of the arrow-head ($n = 8$) obtained by adding one point to the hexagon. ———, hexagon and ------, arrow-head are calculated from Eqn. 10; · · · · · ·, Monte Carlo simulation for the hexagon.

accuracy of this model is not significantly better than that of the empirical formula, and worse in the cases of dimers and triangles (reflecting the inapplicability of the model to not fully symmetric shapes, at least for small n, cf. below).

Given the reliability of the numerical results obtained from Eqns. 9 and 10 together with Eqn. 14, these formulae can now be used to present directly the variations of binding curves as a function of ligand shape. Corresponding model curves are depicted in Fig. 4: Scatchard plots are seen to flatten more and more as the shape changes from that of a linear rod to thicker rods and finally squares.

In the case of very large ligands, Eqns. 9 and 10 may be simplified further. We note first that the exponent γ increases with increasing n, either because the excluded areas become large (as in the case of rods, with λ nearly constant) or because λ tends to zero (as in the case of regular polygons, with α nearly constant). Now, the square-bracket expression on the right-hand side of Eqn. 10 may be rewritten:

$$[\dots]^{-\gamma} = \exp[-\gamma \ln(1 + \lambda nr/(1 - nr))]$$

For large values of γ, this must be very small, except for values of (nr) near to zero. The significant part of a Scatchard plot then falls exclusively into the range of small (nr). Developing the logarithm, we obtain the following simplified version

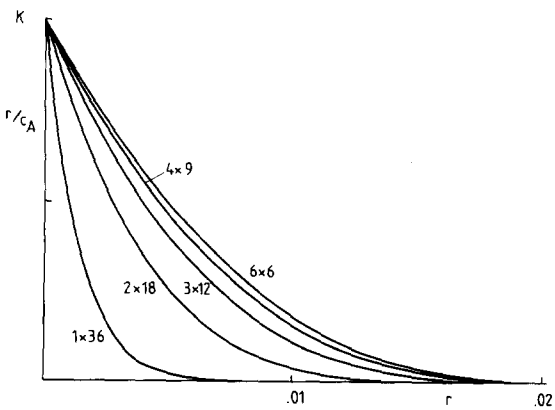

Fig. 4. Binding isotherms of $n = 36$ ligands of different shapes, assumed to be rectangles on a square lattice, with sides as indicated. 1×36 represents the linear ligand, 6×6 the square.

of Eqn. 10 under these conditions:

$$\frac{r}{c_A} = K(1 - nr) \exp\left(-\frac{\alpha nr}{1 - nr}\right) \tag{15}$$

We have checked numerically that Eqn. 15 can be used instead of Eqn. 10 for values of n larger than about 10.

Interestingly, Eqn. 15 is formally equal to the result of the simplified model of Andrews, Eqn. 16 of Ref. 2. In principle, the latter is only valid for symmetric structures. If one nevertheless uses it for other shapes, with the appropriate values of α inserted, deviations from the correct binding curves occur mainly at moderately large (nr), cf. Fig. 2. Provided that n is large enough, this range is of no practical relevance, because it corresponds to the very flat portion of the isotherms (or, in Scatchard representations, to nearly vanishing r/c_A), which again establishes the applicability of Eqn. 15.

Cooperativity

In cooperative systems, the binding affinity of a ligand is modified by the presence of other, already bound ligand molecules. Different forms of cooperativity may exist, for example, long or short range interactions, interactions depending on the mutual orientations of the bound molecules, etc. Here, we propose a model of nearest-neighbour cooperativity without orientational effects; the cooperative interaction is assumed to increase with increasing length of the contact region between bound ligands. Such a concept can be incorporated into the formalism so far developed in a quite natural way [14].

In the framework of the Miller-Guggenheim theory, the relevant information is contained in the pair distributions. To introduce cooperativity, we therefore assume that the binding strength of a ligand depends on the number of pair interactions which it forms with neighbouring molecules. Since each ligand molecule makes $zn\lambda$ pair contacts with its nearest-neighbour shell [1], there are as many molecular binding constants $(K_b)_i$ $(i = 1, \dots, zn\lambda)$. Each of them refers to an elementary reaction of a ligand binding to a free site in such a way that i bound-bound pairs are formed. Thus, $(K_b)_i$ equals the probability of finding a bound

site with an environment i (i.e., i bound-bound pairs and $(zn\lambda - i)$ bound-free pairs at the edges), divided by the probability of finding a free site with the same environment (i.e., i free-bound pairs and $(zn\lambda - i)$ free-free pairs at the edges). More explicitly:

$$K_i c_A = \rho \frac{r}{x_{(n)}} \left(\frac{x_{22}^e}{\lambda x_2}\right)^i \left(\frac{x_{12}}{\lambda x_2}\right)^{zn\lambda - i} \left(\frac{x_{11}}{x_1}\right)^{-i} \left(\frac{x_{12}}{x_1}\right)^{-zn\lambda + i} \tag{16}$$

where the conditional probabilities written in parentheses should be obvious from considering Eqns. 2a and 3. For example, $x_{22}^e/\lambda x_2$ represents the probability of having a bound-bound pair formed between two neighbouring ligand molecules (x_{22}^e), if it is already known that one subunit is bound and lies at the edge of a ligand (λx_2). Of course, lattice points in the interior of a region bound by a ligand molecule play no role because they are not statistically independent. This is why x_{22}^e and λx_2 appear, instead of x_{22} and x_2. The other conditional probabilities follow in the same way, and the total probability is found by multiplying the individual pair probabilities. Furthermore, in Eqn. 16, we have turned to effective binding constants, K_i, by multiplying with the statistical factor ρ.

Comparing the molecular binding constants at different environments i and taking into account that $x_{11}x_{22}^e/x_{12}^2$ equals η, the cooperativity parameter (Eqn. 4), the various binding constants K_i are found to be related by $K_i = \eta\, K_{i-1}$, or else:

$$K_i = \eta^i K_0 \tag{17}$$

with K_0 being the binding constant on a site completely surrounded by free subunits. Therefore, once any of the K_i is known, the others follow immediately by means of Eqn. 17.

It is convenient to formulate the following for the case where half of the nearest-neighbour shell is free, the other half occupied by bound ligand, i.e., $i = zn\lambda/2$. For the sake of simplicity, $zn\lambda/2$ will be denoted by δ and the corresponding binding constant K_δ simply by K, without any subscript.

Eqn. 16 may be rewritten by taking the case of random adsorption as the reference state (the corresponding quantities being marked by an asterisk):

$$Kc_A = \frac{r}{x_{(n)}} \left[\frac{x_{22}^e}{x_{22}^{e*}} \frac{x_{11}^*}{x_{11}}\right]^\delta \tag{18}$$

with $x_{11}^* = x_1^2/(x_1 + \lambda x_2)$, $x_{22}^{e*} = \lambda^2 x_2^2/(x_1 + \lambda x_2)$ or else, using Eqns. 5 and 6:

$$x_{11}/x_{11}^* = 1 + Ap$$

$$x_{22}^e/x_{22}^{e*} = 1 + A/p$$

$$A = (\sqrt{\gamma} - 1)/(\sqrt{\gamma} + 1)$$

$$p = \lambda nr/(1 - nr) \tag{19a,b,c,d}$$

The symbol $\sqrt{\gamma}$ is the same as the one defined in Eqn. 6, with $x_2 = nr$.

The expression for $x_{(n)}$ has been obtained before (cf. Eqn. 7) and may be inserted into Eqn. 18 to yield, after some simple rearrangements:

$$Kc_A = B_0(1 + A/p)^\delta (1 + Ap)^{-\gamma - \delta} \tag{20}$$

B_0 represents the right-hand side of Eqn. 9. Similarly, in the Scatchard representation:

$$r/c_A = C_0(1 + A/p)^{-\delta}(1 + Ap)^{\gamma + \delta} \tag{21}$$

where C_0 stands for the right-hand side of Eqn. 10 with K interpreted as K_δ. A and p are given by Eqns. 19c, d above.

Eqns. 20 and 21 are fully consistent in the case of linear ligands [14], and are then equivalent to the results obtained by Miyazawa [13]. (In Miyazawa's notation, Eqn. 22 of Ref. 13, q corresponds to our $n\lambda$, γ to our η, and β is our $\sqrt{\gamma}$.)

Fig. 5 shows the effect of cooperativity as calculated by means of the above formulae: the downward curvature of Scatchard binding curves is reduced and, at large cooperativity, even overcompensated so that the Scatchard plot describes a hump [6]. Such a behaviour is completely analogous to the one known from linear systems, for example, unspecific protein binding to DNA [15]. In fact, the one-dimensional treatment is contained as a special case in Eqns. 20 and 21, and may be rederived by setting $z = 2$, $\gamma = n - 1$, $\lambda =$

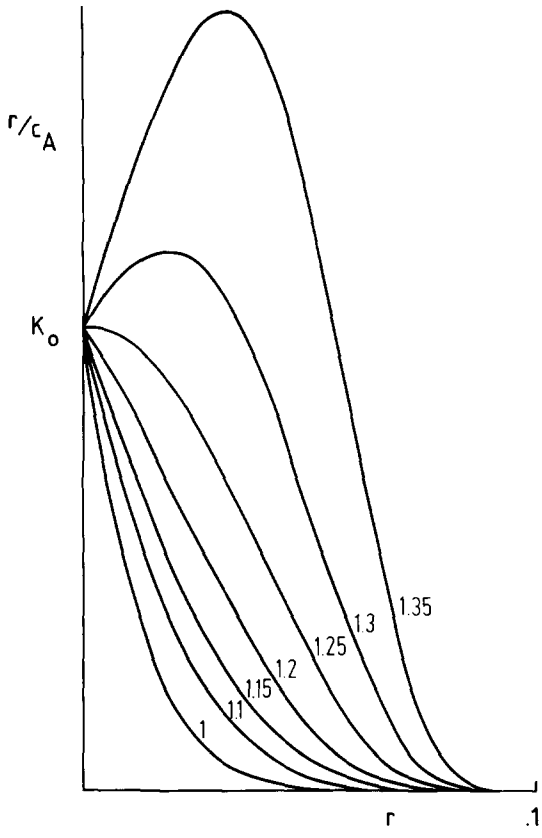

Fig. 5. Binding isotherms for an $n = 10$ linear ligand with different degrees of (positive) cooperativity (in the sense defined by the Guggenheim model). The values of the cooperativity parameter η are indicated. $\eta = 1$ corresponds to random adsorption (no cooperativity). Anticooperativity would not compensate but accentuate the concave curvature.

$1/n$ and $\rho = 1$ (i.e., $K = K_b$; comparing with Eqn. 15 of Ref. 15, note that their K corresponds to our K_0; correspondences of the other symbols are: $\omega = \eta$, $\nu = r$ and $R = [1 - (n-1)r]\sqrt{\ }$; the factor $2\omega + 1$ in the first numerator on the right-hand side should read $2\omega - 1$).

In the spirit of what has been said in the section on nonlinear ligands, the result, Eqns. 20 and 21, can also be extended in an empirical way to other ligand shapes, using the appropriate definition of γ (Eqn. 14) in terms of the excluded area.

From considering Scatchard plots, it is evident that the effects of cooperativity (tendency for convex or upward curvature) compensate those of large size and/or extended shape (tendency for concave or downward curvature). Quantitative information may be drawn from the expression for the initial slope of a Scatchard plot:

At vanishing saturation, $(1 + Ap)$ tends to unity, $(1 + A/p)$ tends to η, and the remaining of the right-hand side of Eqn. 21 to K. Thus, the ordinate intercept of the Scatchard plot, I_0, is:

$$I_0 = K/\eta^\delta = K_0 \tag{22}$$

as in the noncooperative case. Taking derivatives with respect to r yields the initial slope, S_0:

$$S_0 = -nK_0[1 + \gamma\lambda - zn\lambda^2(\eta - 1)] \tag{23}$$

The initial slope becomes positive, leading to a hump in the Scatchard plot, if:

$$\eta > 1 + (1 + \gamma\lambda)/(zn\lambda^2)$$

For example, for $n = 7$ hexagons on a hexagonal lattice ($z = 6$, $\gamma = 4$, $\lambda = 3/7$), this occurs for $\eta > 1.352$. For a linear rod with $n = 7$, the corresponding condition reads $\eta > 1.247$. At first sight, it might seem paradoxical that the limiting η value for the linear rod is smaller than that for the hexagon, since in the latter case cooperativity has to compensate for a weaker tendency of downward curvature. But on the other hand, the linear rod makes more nearest-neighbour contacts – as reflected by the larger value of $\lambda = 5/7$ – which serve to potentiate the interaction. In order to account for such shape effects, one may consider η^δ when comparing ligands of different shapes. The condition for positive initial slope would then read $\eta^\delta > 15.1$ for the $n = 7$ hexagon, and $\eta^\delta > 27.3$ for the $n = 7$ rod. η^δ is also the factor by which $K = K_\delta$, the binding constant for cooperative growth at half-bound environment, is larger than K_0, the binding constant for an isolated ligand.

Discussion

The present article completes a series of reports in which we attempt to give a description of large-ligand adsorption to membranes, with special emphasis on steric effects. In doing this, we have tried to reduce the mathematical complexity to a minimum, by using suitable approximations.

The precision of these approximations has been demonstrated to be fully sufficient for practical purposes (cf. the comparison with Monte Carlo simulations in Fig. 2). The treatment is general enough to be applied to a variety of different experimental situations to be discussed in the following.

Noncooperative large-ligand adsorption

Some aspects of this problem have already been dealt with previously [1,2]. Here, the treatment is completed to include a broad class of ligand shapes. For the first time, to our knowledge, formulae are made available which allow a general discussion of the binding of various types of large ligands (Eqns. 9 and 10 and Fig. 4).

Analysis of the numerical results obtained with these equations indicates that in many practical situations, the general formulae may be replaced by even simpler expressions. For instance, if the ligands are so large that each molecule covers at least ten binding contacts on the membrane, binding isotherms can be calculated by means of Eqn. 15. Three parameters are needed: the effective binding constant K (equal to the molecular binding constant times the number of distinct orientations of the ligand on the lattice, ρ), the stoichiometric number n, and the excluded-area parameter α, which reflects the shape dependence and has been tabulated for a large class of different shapes in Appendix 1. r is the concentration of bound ligand per total concentration of binding contacts.

Eqn. 15 has previously been derived for the special case of bulky ligands with fully symmetric shapes (e.g., squares on a square lattice, hexagons on a hexagonal lattice, etc.). It turns out to remain valid, however, for arbitrary shapes, provided n is large enough ($n \gtrsim 10$) and the correct value of α is inserted. An explanation for this astonishing result is given at the end of the section on 'non-linear ligand shapes'. (Concerning the discrepancies at small n, cf. the $n = 2$ curve in Fig. 2 and the argument at the end of Discussion in Ref. 2.)

In the present article, Eqn. 15 has been derived in a completely different way, starting from the linear-ligand treatment of Miller and Guggenheim which was extended in an empirical way in order to account for nonlinear ligands, too. The resulting formula, Eqn. 10, can be developed for n larger than about 10 to yield again Eqn. 15.

It is important to notice that isotherms in the form of Eqn. 15 are independent on whether one assumes adsorption to a lattice of point contacts or to a surface continuum (cf. Ref. 2). In the latter case, it is advantageous to replace (nr) by a, the fraction of membrane area covered by bound ligand:

$$r/c_A = K(1-a)\exp[-\alpha a/(1-a)] \qquad (24)$$

Eqn. 15 remains valid for arbitrary n in the case of fully symmetric ligands.

Despite the simple mathematical form of the isotherms for very large ligands ($n \gtrsim 10$), the evaluation of experimental binding curves is complicated by the strong dependence on the shape of the ligand [2]. The latter enters through the parameter α. Shape dependence has been demonstrated to be less drastic for smaller ligands [2]. If the shape is known, however, it may be taken into account explicitly by means of our empirical extension of the linear-ligand treatment (Eqns. 9 and 10) with γ reinterpreted as $\gamma = \alpha/\lambda$). In these equations, a second geometrical parameter, λ, appears which is easy to determine [1] and tabulated together with α in Appendix 1. The full physical importance of this parameter will only be appreciated when discussing cooperativity. For a given ligand shape, α and λ are purely theoretical quantities and no fit parameters.

If the ligand shape is not known beforehand, it will generally be difficult to extract the relevant information from the binding curves alone. However, with accurate data in hand, one may at least exclude some extreme shapes, as demonstrated in Fig. 6a: it is impossible to fit a linear-rod isotherm to the binding curve of a 5×5 square, by simple variation of n. In order to get the correct initial slope of the rod, its length must be assumed so small that deviations of the corresponding isotherm occur at moderate saturation. The situation is more difficult if n is smaller than or in the range of 10 (Fig. 6b): isotherms of an $n = 6$ rod and of a 2×4 rectangle are close to each other (as well as those of an $n = 8$ rod and a 3×4 rectangle), though the 3×3 square remains quite distinct.

On hexagonal lattices, mathematical simplifications are possible for small ligands ($n \lesssim 10$) too.

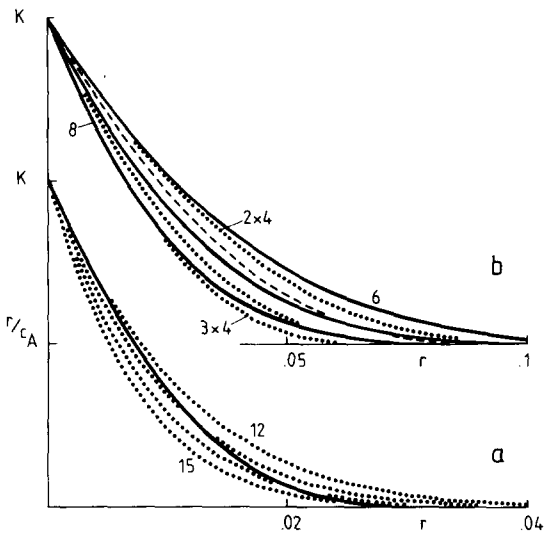

Fig. 6. (a) Comparison of binding isotherms of a 5×5 square (———) and linear rods (· · · · · ·) of varying length n as indicated, on a square lattice. It is impossible to fit the square with a rod isotherm. (b) The same for a 3×3 square (------), 2×4, 2×5 and 3×4 rectangles (in the order of increasing steepness, · · · · · ·) and $n = 6$, 7 and 8 linear rods (in the order of increasing steepness, ———), on a square lattice.

They can be treated quite accurately by means of the simple Bragg-Williams approximation [1]:

$$r/c_A = K(1 - nr)^n \tag{25}$$

This formula is equivalent to a simple mass-action law. (The spatial coordination of the contacts forming the binding site is neglected.) Such a formula has been used, for instance, to analyse the binding of divalent and trivalent ions to lipid membranes [16]. Note that the nth power form in Eqn. 25 arises simply from counting free sites correctly and has nothing to do with the question whether the lipid headgroups, considered as the binding contacts in these studies, are thought to form a rigid lattice or to be able to diffuse around [16].

Cell receptor binding

Diffusion of binding contacts may become important, on the other hand, if the binding subunits are not close-packed (as the lipid headgroups in lipid-protein adsorption which has motivated this work), but rather dilute in the surface, i.e., if their mutual distance is not small with respect to the size of the ligand. Such a situation may occur, for instance, in some cases of receptor binding where the unbound receptors are far apart from each other and start to diffuse together and to form clusters only upon binding of the ligand.

Of course, it cannot be the scope of this article to give a general account of the variety of mechanisms which may be relevant in cell receptor binding, especially as there remain many open questions about the details of receptor clustering. We only want to point out that the formalism presented so far can readily be generalized by separating the contributions of excluded areas, on one hand, and the counting of free sites, on the other hand:

If the free receptors are far apart from each other, their spatial arrangement does not matter and they may be considered as being statistically independent. Therefore, the counting of free sites is adequately done by means of the simple nth power Bragg-Williams term (mass-action law): $x_{(n)} = (1 - nr)^n$. The probability of finding n free receptors, $x_{(n)}$, has then to be multiplied by the probability of finding a free place on the membrane, i.e., one which does not overlap with any of the excluded areas of the already bound ligands. The latter probability is given, in a continuum approach, by the exponential term of Eqn. 15. (Clearly, α has to be calculated in terms of surface units and not in terms of receptor-binding contacts). Thus, binding to dilute receptors is governed by the following equation:

$$r/c_A = K(1 - nr)^n \exp[-\alpha a/(1 - a)] \tag{26}$$

The surface fraction occupied by bound ligand, a, is of course still proportional to r, but the proportionality coefficient is no longer simply n (instead, it equals the area covered per ligand molecule, divided by the total surface area per receptor). Note that the area covered is intended to mean the area made unavailable for further ligand binding. For example, in the case of antibody binding to haptens ($n = 2$), this area should include approximately the whole stretch of surface lying in the line between the two bound haptens, in order to account for the excluded volume of the antibody.

The exponential term in Eqn. 26 will be rele-

vant only at comparatively high membrane saturation. In any case, the treatment refers to equilibrium binding only and cannot be applied to situations which are governed by kinetic processes (as studied, e.g., in Ref. 17). Nevertheless, we think that the concepts worked out here may also prove useful in constructing kinetic models which account adequately for the steric properties of large ligand molecules.

Cooperative binding

The Miller-Guggenheim method allows a simple extension to the case where the binding affinity is modified by nearest-neighbour interactions between bound ligand molecules. In this mathematically simple model, cooperative interactions of equal strength are thought to arise at all contacts between bound molecules. The resulting isotherms, Eqns. 20 and 21, contain a single new parameter, the cooperativity parameter η defined in Eqn. 4. In Eqns. 20 and 21, $K = K_\delta$ is to be interpreted as the effective binding constant on a site surrounded to one-half by free subunits and to the other half by bound subunits. This situation can be identified with the cooperative growth at the border of a large cluster. The effective binding constant for an isolated ligand molecule is then given by $K_0 = K/\eta^\delta$. Thus, $\eta > 1$ corresponds to positive cooperativity (tendency for cluster formation), $\eta < 1$ to anticooperativity (tendency for isolation of individual ligand molecules), and $\eta = 1$ to random adsorption.

Relatively small variations of η away from unity (e.g., $\eta = 1.2$) are already sufficient to induce substantial cooperative effects, due to the potentiation of the interaction by the large number of nearest neighbours. In Scatchard plots, positive cooperativity results in a compensation of downward curvature which may even lead to a characteristic hump, if η is large enough (cf. Fig. 5). The quantitative condition for such a behaviour is found from considering the initial slope, S_0.

Eqn. 20 is equivalent, in the case of linear-ligand binding, to the results obtained in a more formal way by Guggengeim [14] and, more recently, by Miyazawa [13]. Setting $z = 2$, one recovers the well-known formula of Mc Ghee and Von Hippel [15] for large-ligand binding to linear polymers, such as DNA.

Eqns. 20 and 21 can also be applied to nonlinear ligand adsorption just in the same way as discussed above for random adsorption. In general, reasonable assumptions about the ligand shape appear to be a prerequisite for such applications, because otherwise, the number of free parameters (binding constant, cooperativity, ligand size and shape) will exceed the limit where they can be separated without ambiguity. For n smaller than about 10, however, we find again from numerical analysis that rough, but reasonable parameter estimates can be obtained with essentially arbitrary shape assumptions. There seems thus to be a compensation between the larger steric effects of extended ligands, on one hand, and their stronger potentiation of cooperativity due to a larger number of nearest neighbours, on the other hand. For the sake of demonstration, we have reevaluated published data of the cooperative binding of polymyxin to phosphatidic acid bilayers.

Example: Polymyxin binding to membranes

Binding of the antibiotic polymyxin B to negatively charged phosphatidic acid bilayers has been studied by (among others) Hartmann and coworkers [18]. We chose to fit their experimental curve in Fig. 7 of Ref. 18. Cooperativity of binding is evident from the sigmoidal shape of the binding isotherm. The curve flattens at a concentration ratio of about 5 : 1 total peptide/lipid. Clearly, a considerable amount of peptide must be unbound at these concentrations, so the stoichiometric number has to be definitely larger than 5. In addition, large-ligand binding curves tend to flatten well below complete saturation. Therefore, we fitted our model directly to the experimental curve, taking the scale of the ordinate as an additional fit parameter. The lipid membrane was represented by a hexagonal lattice ($z = 6$).

The best fit was obtained when we modeled the shape of polymyxin (a cyclic ring with a linear tail, cf. Fig. 8 of Ref. 18) by an $n = 7$ hexagon with a linear protrusion 2 subunits long. This structure has the following geometrical parameters: $n = 9$, $\alpha = 92/27$, $\lambda = 13/27$. Using $K_0 = 370\ \mathrm{M}^{-1}$ and $\eta = 1.72$ as the cooperativity parameter, the fit curve deviated from the experimental curve nowhere more than the thickness of the line trac-

ing in the figure in Ref. 18. (Unity on the ordinate axis was then replaced by 0.86).

Very good fits could also be obtained by assuming a linear ligand shape, with $n = 8$, $K_0 = 280$ M^{-1}, $\eta = 1.59$, and a compact shape with $n = 10$, $K_0 = 530$ M^{-1}, $\eta = 1.67$. (In the latter case, we could not avoid slight deviations from the experimental curve at very low peptide concentrations; these were still so small, however, that it would be difficult to represent them on the scale of an ordinary figure).

We conclude from this analysis, that the shape-dependence remains small enough for $n \lesssim 10$, even in cooperative systems, so that the results may be used at least as reasonable estimates, for any assumption about ligand shapes. As for the cooperativity parameter, this statement remains only true as long as one considers η itself, and not η^{δ} (the latter being 1153, 2653 and 786, respectively, for the three fits mentioned above).

Comparing our approach to the Bragg-Williams-type treatment leading to the calculated curve of Fig. 7 of Ref. 18, it should be recognized that the latter does not account for the size of the ligand (i.e., not even for the lipid : ligand stoichiometry). As it stands, this treatment would be valid for the 1 : 1 adsorption of small ligands. In principle, the cooperative energy (exchange energy) parameter w as used in Ref. 18 is related to our η by $w = kT \ln \eta$.

Protein incorporation into membranes

Being concerned with the adsorption of biological ligands, for example, proteins, to membranes, it must be recognized that in many cases of practical interest, the ligand is not only attached to the membrane but also anchored by inserting some parts more or less deeply into the lipid core. This happens, for instance, with melittin, the binding of which was discussed in Ref. 1. It is important to assess to what degree the binding isotherms might be affected by such mechanisms.

To do this, we take advantage of the fact that the present formalism can be readily restated in terms of protein incorporation into membranes. In Appendix 2, we give the relevant formulae for the adsorption of a protein with concomitant incorporation. In principle, this formalism can be used for treating a variety of problems connected with protein incorporation and protein distribution in membranes. Here, we limit ourselves to state the result that membrane insertions can simply be neglected in the evaluation of binding curves as long as they remain small with respect to the area of the bound lipids. This comes out of model calculations such as the following example. We compared binding curves for a ligand adsorbing to 12 lipids in two different situations: (1) without incorporation, assuming a rectangular shape of 2×6 subunits on a square lattice; (2) with a central part of 3 subunits incorporated and the nearest-neighbour shell (the circumference of a 3×5 square) bound. The affinity constant was taken to be the same in both cases. Applying Eqn. A-16 (with $n' = 12$ and $n'' = 0$ and 3 for the two cases, respectively), the resulting isotherms were found to be very close to each other (not shown), indicating that the 20% membrane insertion (3 subunits versus 12 bound subunits) did not significantly affect the binding curves.

Conclusions

Useful treatments for the adsorption or incorporation of linear-chain molecules have long been known (e.g., Ref. 14). From practical applications to membrane research, we have recognized, however, that these models are of limited use for a broad range of biochemical and biophysical work, because they cannot account for the strong shape-dependence. Physical chemists can normally circumvent this problem by using virial expansions for dilute polymer solutions [19,2]. With biological membranes, such an approach does not help very much, because the protein content or saturation with ligand are often so high that any expansion approach must break down.

Though we have not been able to solve this problem once and for all, we think it is a great advantage to have formulae at hand (Eqns. 9, 10 and 15 or Eqns. 20 and 21 in the cooperative case) which allow to treat adsorption of large ligands of essentially any shape, with or without cooperativity. From a theoretical point of view, it may be less satisfactory that the most general formulae have not been derived in a rigorous way. However, they have been shown to yield reliable results, the parameters used are well-defined and have a precise physical meaning, and the equations go over

to consistent expressions in the limits of extreme shapes (stretched linear ligands and large bulky ligands).

Appendix 1

In this Appendix, we give the relevant expressions for the geometrical parameters α and λ to be used in Eqns. 9 and 10, Eqn. 15 or Eqns. 20 and 21 for ligands of various shapes. The parameter γ appearing in some of these equations is simply given by $\gamma = \alpha/\lambda$. In all examples, the structures are thought to correspond to the shape of the surface region covered by an individual ligand molecule upon adsorption. The notion of length is in terms of the number of lattice points covered. The structures to be treated are represented in Fig. 7. In the following, numbers given in parentheses refer to the labelling of this figure.

For the sake of notational simplicity, most formulae are given in implicit form as a function of geometrical parameters like side-lengths, etc. Expressing these parameters as functions of the stoichiometric number n, α and λ are obtained as functions of n, too. (In the case of rectangles, sides a and b may be expressed as functions of n and the axial ratio $p = a/b$, cf. Ref. 2). Thus, with a given shape assumption, the resulting binding formulae depend on the binding constant K and the stoichiometric number n.

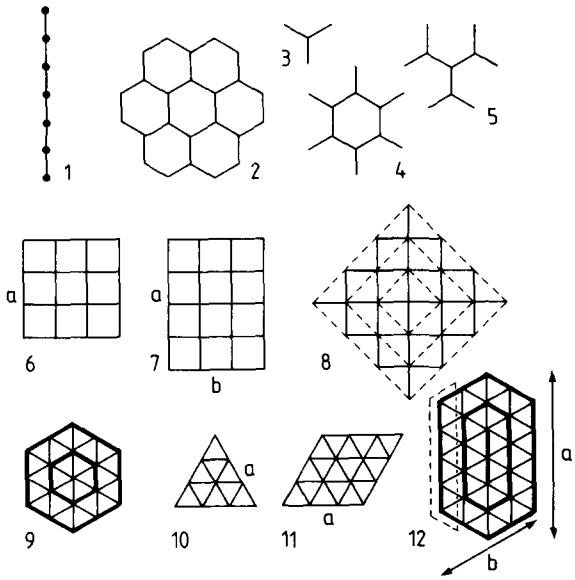

Fig. 7. Geometrical structures treated in Appendix 1. (1) Linear rod, $n = 7$; (2) hexagons, $k = 2$; (3) Y, (4) star; (5) tree; (6) square, $a = 4$; (7) rectangle, $a = 5$, $b = 4$; (8) oblique square, $k = 3$ (dashed lines indicate contours of square shells and are not bond lines); (9) hexagon, $k = 2$ (shells indicated by heavy lines); (10) triangle, $a = 4$; (11) rhombus, $a = 4$; (12) stretched hexagon, $a = 7$, $b = 5$ ($p = 2$, $k = 3$; heavy lines indicate shells defining k and p); elimination of the part enclosed by dashed lines yields a structure with $a = 7$ and $b = 4$ ($k = 3$, $p = 3/2$).

(1) The formulae for linear rods can be stated in closed form for any lattice of contacts [1,2]:

$$\lambda = (z-2)/z + 2/(zn)$$

$$\alpha = (n-1)\lambda \qquad \text{(A-1)}$$

The remaining structures have to be considered in terms of the underlying lattice:

A. Honeycomb lattice ($z = 3$)

(2) Honeycomb hexagons, made up of k concentric shells of hexagons, the central hexagon corresponding to $k = 1$:

$$n = 6k^2,\ k = (n/6)^{1/2}$$

$$n\lambda = 2k$$

$$n\alpha = 2(3k-1)^2 \qquad \text{(A-2)}$$

(3) $n = 4$ Y:

$$\lambda = 1/2,\ \alpha = 3/2 \qquad \text{(A-3)}$$

(4) $n = 12$ star: hexagon with protruding bond lines:

$$\lambda = 1/3,\ \alpha = 13/6 \qquad \text{(A-4)}$$

(5) $n = 10$ tree: Y with protruding bond lines at each end:

$$\lambda = 2/5,\ \alpha = 21/10 \qquad \text{(A-5)}$$

B. Square lattice ($z = 4$)

(6) Square, side of length a:

$$n = a^2,\ a = n^{1/2}$$

$$n\lambda = a$$

$$n\alpha = (3a-1)(a-1) \qquad \text{(A-6)}$$

(7) Rectangle, sides a and b:

$$n = ab$$

$$n\lambda = (a + b)/2$$

$$n\alpha = [(a-1)(a+1)+(b-1)(b+1)+4(a-1)(b-1)]/2 \quad \text{(A-7)}$$

(8) Oblique square (edge 45° to lattice axes), k concentric shells around central point (cf. dashed lines in Fig. 7):

$$n = 1+2k(k+1),\ k = \left(-1+[1+2(n-1)]^{1/2}\right)/2$$

$$n\lambda = 2k+1$$

$$n\alpha = 2k(3k+1) \quad \text{(A-8)}$$

C. Hexagonal lattice (z = 6)

(9) Regular hexagon, k concentric shells around central point:

$$n = 1+3k(k+1),\ k = \left(-1+[1+4(n-1)/3]^{1/2}\right)/2$$

$$n\lambda = 2k+1$$

$$n\alpha = 3k(3k+1) \quad \text{(A-9)}$$

(10) Equilateral triangle, side of length a:

$$n = a(a+1)/2,\ a = \left(-1+[1+8n]^{1/2}\right)/2$$

$$n\lambda = a$$

$$n\alpha = (4a-1)(a-1)/2 \quad \text{(A-10)}$$

(11) Rhombus, side of length a:

$$n = a^2,\ a = n^{1/2}$$

$$n\lambda = (4a-1)/3$$

$$n\alpha = (11a-5)(a-1)/3 \quad \text{(A-11)}$$

(12) Stretched hexagon (formed by a straight line of length k with p contour shells around it; the resulting hexagon has an overall length $a = k + 2p$ and breadth $b = 2p + 1$, cf. Fig. 7):

$$n = a(1+2p)-p(p+1)$$

$$n\lambda = [2(a+p)+1]/3$$

$$n\alpha = [2a^2-p^2+10ap-7p-a-1]/3 \quad \text{(A-12)}$$

Eqn. A-12 can also be used as a very good approximation for the less regular structures obtained from (12) by cancelling one of the outer columns, thereby reducing the breadth b by one unit ($p = (b-1)/2$ becomes non-integer), as indicated by dashed lines in Fig. 7.

Whereas λ is always easy to determine (counting the bond lines emanating from the structure considered and dividing by zn), the determination of α may be more laborious, though straightforward, according to the recipe given in Ref. 2. In any case, values tabulated above may be used as good approximations for similar structures.

Note that the formalism implicitly assumes that the ligand is able to fully saturate the membrane. This may not be the case for some particular shapes with strongly irregular circumferences (or round shapes such as disks, but this is anyway too idealized to be realistic). Though such properties should affect the isotherms only in the high-saturation regime which is normally of minor experimental importance, an explicit correction is possible along the lines discussed in Ref. 2: replace the $(1 - nr)$ denominator in the exponent of Eqn. 15 by $(1 - wr)$, where $w = 1/r_{max}$ is the reciprocal of the maximum obtainable saturation; similarly, replace the contents of the square brackets of Eqn. 9 by $[(1\text{-}wr + \lambda nr)/(1 - wr)]$.

Appendix 2: Membrane incorporation

The treatment given in this work can be readily reformulated for protein incorporation into membranes. As an example, we shall present the corresponding equations in the case where the lateral distribution of the protein molecules is random.

Again, we consider a two-dimensional lattice, with a lattice constant equal to the average distance between lipid headgroups (or between fatty acid chains or whatever represents the independent unit in the system to be studied). We imagine this lattice to extend over the whole membrane,

not only over those parts actually occupied by lipids, but also over the proteins. Thus, each incorporated protein molecule occupies n lattice points, arranged according to its shape. The equivalence with the adsorption problem becomes evident if we identify x_1 with the fraction of lattice points occupied by lipid and x_2 with that fraction occupied by protein. One difference exists, however, with respect to adsorption, namely that the total number of subunits, N, is no longer constant but increases with increasing protein content of the membrane.

Let N_1 be the number of lipids and N_2 be the number of proteins in the membrane. The total number of subunits is then $N = N_1 + nN_2$, and the fractions of subunits occupied by lipid and protein are $x_1 = N_1/N$ and $x_2 = nN_2/N$, respectively. The concentration of protein incorporated per lipid, ν, becomes:

$$\nu = N_2/N_1 = r/(1 - nr) \tag{A-13}$$

if we continue to define $r = x_2/n$, as before.

In the case of adsorption considered in the main part, $K_b c_A$ equals the quotient of the activities of bound complex and of free subunits, or else

$$RT \ln K_b c_A = \Delta\mu_2 - n\Delta\mu_1$$

$\Delta\mu_2$ and $\Delta\mu_1$ being the nonstandard parts of the chemical potentials of ligand-covered and ligand-free subunits. To establish the equivalence with membrane incorporation, $\Delta\mu_2$ and $\Delta\mu_1$ have to be reinterpreted in terms of chemical potentials of protein and lipid, respectively. Of course, the affinity constant for incorporation, K_b^{inc}, only refers to $\Delta\mu_2$ ($RT \ln K_b^{inc} c_A = \Delta\mu_2$), and we must thus extract the corresponding contribution from the total expression (9). To do this, we imagine Eqn. 9 to result from differentiating the nonstandard part of the Gibbs free enthalpy with respect to N_2, N being held constant. $\Delta\mu_2$ can therefore be obtained by integrating the expression for $\ln K_b c_A$ (i.e., the logarithm of the right-hand side of Eqn. 9 after division by ρ) with respect to $N_2 = rN$, at constant N, and subsequently differentiating with respect to N_2, at constant N_1:

$$\frac{\Delta\mu_2}{RT} = \ln\frac{r}{\rho} - \frac{\gamma\lambda}{1-\lambda}\ln[1-(1-\lambda)\,nr] \tag{A-14}$$

This should equal $\ln K_b^{inc} c_A$. Inserting the degree of incorporation, ν, from Eqn. A-13, we obtain the following isotherm (with $\rho K_b^{inc} = K_{inc}$):

$$K_{inc} c_A = \frac{\nu}{1+n\nu}\left[\frac{1+n\nu}{1+\lambda n\nu}\right]^{\gamma\lambda/(1-\lambda)} \tag{A-15}$$

We can even go one step further and consider the incorporation of a protein which, upon insertion into the membrane, binds n' lipids. One membrane protein then effectively blocks n subunits, n' of which are bound lipids and the remainder $n'' = n - n'$ occupied by the protein itself.

As before, $RT \ln K_b^{inc} c_A$ must equal $\Delta\mu_2 - n'\Delta\mu_1$. By a similar procedure as the one described above, we find, with $\nu = N_{prot}/N_{lip} = r/(1 - n''r)$:

$$K_{inc} c_A = \nu(1+n''\nu)^a(1-n'\nu)^b(1-n'\nu+\lambda n\nu)^c \tag{A-16}$$

with

$$a = -(n''/n)[1-\lambda(\gamma+1)]/(1-\lambda)$$

$$b = -(\gamma+1)n'/n$$

$$c = (n'/n-\lambda)\gamma/(1-\lambda) \tag{A-17a, b, c}$$

Note that for $n'' = 0$ ($n' = n$) this formula reduces to Eqn. 9 for simple adsorption without incorporation, as it should.

The corresponding formulae become quite complex in the most general case with cooperative interactions. Here, we restrict ourselves to the special case of linear-ligand incorporation without lipid binding; we then get [14]:

$$K_{inc} c_A = \frac{\nu}{1+n\nu}\left[\left(1+\frac{A}{\lambda n\nu}\right)\frac{1+n\nu}{1+\lambda n\nu}\right]^{\delta} \tag{A-18}$$

with A and λ given by Eqns. 19c and A-1, respectively, and $\delta = zn\lambda/2$. Since A tends to zero as the cooperativity parameter approaches unity, Eqn. A-18 clearly goes over to Eqn. A-15 in the limit of random adsorption (note that $\delta = \gamma\lambda/(1-\lambda)$ for linear ligands).

References

1 Stankowski, S. (1983) Biochim. Biophys. Acta 735, 341–351
2 Stankowski, S. (1983) Biochim. Biophys. Acta 735, 352–360

3 Cohen, J.A. and Cohen, M. (1981) Biophys. J. 36, 623–651
4 Scatchard, G. (1949) Ann. N.Y. Acad. Sci. 51, 660–672
5 Rosenthal, H.E. (1967) Anal. Biochem. 20, 525–532
6 Schwarz, G. (1976) Biophys. Struct. Mech. 2, 1–12
7 Guggenheim, E.A. (1944) Proc. R. Soc. (Lond.) A183, 203–212
8 Andrews, F.C. (1976) J. Chem. Phys. 64, 1941–1947
9 Silberberg, A. (1970) J. Polym. Sci. 30, 393–397
10 Eisenriegler, E., Kremer, K. and Binder, K. (1982) J. Chem. Phys. 77, 6296–6320
11 Evans, J.W., Burgess, D.R. and Hoffman, D.K. (1983) J. Chem. Phys. 79, 5011–5022
12 Tory, E.M., Jodrey, W.S. and Pickard, D.K. (1983) J. Theor. Biol. 102, 439–445
13 Miyazawa, S. (1983) Biopolymers 22, 2253–2271
14 Guggenheim, E.A. (1944) Proc. R. Soc. (Lond.) A183, 213–227
15 Mc Ghee, J.D. and Von Hippel, P.H. (1974) J. Mol. Biol. 86, 469–489
16 Westman, J., Eriksson, L.E.G. and Ehrenberg, A. (1984) Biophys. Chem. 19, 57–68
17 De Lisi, C. and Wiegel, F.W. (1983) J. Theor. Biol. 102, 307–322
18 Hartmann, W., Galla, H.J. and Sackmann, E. (1978) Biochim. Biophys. Acta 510, 124–139
19 Münster, A. (1956) Statistische Thermodynamik, Chapter 22.2, Springer, Berlin